



In Silico Studies on the Phytochemicals from *Aframomum melegueta* Leaves against Key Enzymes as Anti-Alzheimer's Disease Target

**G. Oluwadahunsi^{a,b*}, S. T. Akinwotu^b, T. M. Fadipe^b, O. P. Akintoye^b,
T. J. Omoyajowo^b, E. T. Ologuntere^b and Z. Abdullah^a**

^a Department of Biomedical Sciences, School of Health Sciences, Health Campus Universiti Sains Malaysia, Kubang Kerian, Kelantan, Malaysia.

^b Cognitive Neuroscience & Neuroinformatics group, Department of Biochemistry, Adekunle Ajasin University, Akungba-Akoko, Ondo State, Nigeria.

Authors' contributions

This work was carried out in collaboration among all authors. All authors read and approved the final manuscript.

Article Information

DOI: 10.9734/IJBCRR/2022/v31i130299

Open Peer Review History:

This journal follows the Advanced Open Peer Review policy. Identity of the Reviewers, Editor(s) and additional Reviewers, peer review comments, different versions of the manuscript, comments of the editors, etc are available here: <https://www.sdiarticle5.com/review-history/84242>

Original Research Article

Received 20 December 2021
Accepted 23 February 2022
Published 25 February 2022

ABSTRACT

Traditional medicine has been practiced for ages across the world using plants as a memory booster and in the treatment of neurodegenerative diseases such as dementia and amnesia. The tau, amyloid hypothesis and neuroinflammation hypothesis are major partakers in a combinational approach in the development of therapy against Alzheimer's disease (AD), Acetyl and butyryl cholinesterases inhibitors have been investigated in clinical trials of AD for a very long time. This research involved an *in-silico* approach to study the interactions of phytochemicals in *Aframomum melegueta* leaves with some enzymes that have been reported in the literature which contribute to neuronal death and memory loss associated in AD. In these studies, Curcumin and Lilacin are shown to have a higher glide score than the co-crystallized ligands of either Acetylcholinesterase, Butyrylcholinesterase or GSK-3 β , they also have higher glide scores than AChE inhibitor Rivastigmine. The ADMET/tox properties of our lead compounds (curcumin and lilacin) ranked them as good candidates for AD drug development, as well as possess the highest docking scores against acetylcholinesterase, butyrylcholinesterase and GSK-3 beta suggesting potent compounds in Alzheimer's disease therapy. The pharmacokinetics studies also showed that curcumin and

*Corresponding author: E-mail: gbenga.oluwadahunsi@aaua.edu.ng;

lilacin would pass through the blood brain barrier into the brain. This work is in line with recent multi-dimensional approach in drug development in that a single compound might possess many active groups which can activate/inhibit more than one protein without any toxic effect.

Keywords: AChE; BChE; GSK-3 β ; Alzheimer's disease; molecular docking; curcumin; lilacin.

1. INTRODUCTION

Alzheimer's disease (AD) is the most commonly diagnosed dementia in aging individuals older than 65 years [1], as this disease advances, the symptoms can include problems with language, disorientation (including easily getting lost), mood swings, loss of motivation and behavioral issues. Traditional medicine has been practiced for ages across the world using plants as a memory booster and in the treatment of neurodegenerative diseases such as dementia and amnesia [2].

The tau, amyloid hypothesis and neuroinflammation hypothesis are major partakers in a combinational approach in the development of therapy against Alzheimer's disease [3], therefore research has been focusing on developing effective treatment for AD. *Aframomum melegueta* is a Zingiberaceae family plant spice used widely in Africa [4]. It's an herb whose seeds have traditional usage mostly as a pungent spice to season foods [5]. Acetyl and butyryl cholinesterases inhibitors have been investigated in clinical trials of AD for a very long time [6] while other approaches focus on the discovery and development of anti-inflammatory agents [7].

Acetylcholinesterase (AChE) is a significant therapeutic target for AD [8] which has been well documented in AD patients [9]. Butyrylcholinesterase (BChE) like AChE also regulates metabolism of the neurotransmitter acetylcholine in the brain of humans. BChE is majorly expressed in the glia and white matter in areas that are important in cognition. In AD, BChE is also linked to the pathologies observed around the cerebral cortex where it's not found predominantly in normal brains [10]. Glycogen Synthase Kinase-3 Beta (GSK3 β) is expressed predominantly in the Central Nervous System, and it is the main kinase involved in the phosphorylation of tau protein whose activity increases in AD cases [11] leading to alterations in axons transport and neurodegeneration in the hippocampus [12].

Molecular docking has become an increasingly important tool for drug [13, 14]. It is a scientific

method that predicts the preferred orientation of a molecule bound to another forming a stable complex [15], the science of the more favorable orientation may then be used to make a prediction of the strength of the association between these two molecules using scoring functions, as molecular docking is one of the methods which is frequently used in the structure-based drug design.

There are changes in AD that involves the cholinergic pathways in the brain especially in the cerebral cortex and hippocampus as these regions have been reported to be involved in memory and other cognitive modelling. Pathological changes in these parts of the brain have been reported to involve decrease in the concentrations of acetylcholine by the enzyme acetylcholinesterase (AChE). AChE inhibitors block AChE which leads to decrease in breaking of acetylcholine.

Rivastigmine has been reported to be an inhibitor of AChE and butyrylcholinesterase therefore making acetylcholine to be available as a neurotransmitter in the brain regions [16].

This study involves an *in-silico* approach to study the interactions of some enzymes that have been reported in the literature to contribute to neuronal death and memory loss associated to AD and phytochemicals in *Aframomum melegueta* leaves. This has emerged as a reliable, cost-effective and timesaving technique for the discovery of lead therapeutic compounds.

2. MATERIALS AND METHODS

Schrodinger suites software (version 2017-1)) was used as the computational tool for this study.

2.1 Protein Preparation

The 3D structures of acetylcholinesterase (PDB :4MOE), butyrylcholinesterase (PDB: 6EP4) and GSK-3 beta (PDB: 4ACC) were all retrieved from the online database (www.rcsb.org/pdb/home.do). These structures were chosen due to their high resolution. The

proteins were imported to maestro interface for the preparation procedure, this was carried out with the protein preparation wizard [17] where missing side chains, loops were filled with prime, missing hydrogen and bond orders were added. The proteins were prepared at neutral pH of 7 ± 2.0 and Het states were generated for the co-crystallized ligands at the active sites of the proteins of interest during the pre-process. Unnecessary water molecules and interfering ligands were removed from the proteins using the review and modify tab followed by H-bond assignment using PROKA to optimize the crystal structure and Restrain minimization at RMSD 0.3 Å with OPLS3 force-field [18].

2.2 Preparation of Ligands

In this study, phytochemicals from *Aframomium melegueta* leaves were retrieved from literature [19]. Rivastigmine (a known AChE inhibitor) was adopted as the reference ligand and its molecular interaction vis a vis docking score pattern was compared to that of *Aframomium melegueta* leaves phytochemicals. The 2D structures of the phytochemicals were retrieved from PubChem database in sdf format and the ligands were prepared with the ligand preparation tool implemented in Schrodinger suite (LigPrep, Schrödinger, 2017-1). The ligands were prepared at a pH of 7 ± 2.0 using an OPLS3 force field, desalt and generate were selected and the stereoisomer was allowed to keep the specific chirality so as to generate maximally thirty-two ligands.

2.3 Anti-AD Molecule (Rivastigmine) used as Control

The 3D structure of Rivastigmine was downloaded from protein data bank and docked into the active site of anti-AD target enzymes, the glide scores will be compared to that of compounds from *Aframomium melegueta* leaves.

2.4 Grid Coordinate of the Receptor

The interaction between ligands and proteins occurs at the active site, areas around this region define the binding pocket in x, y, z coordinates. In the maestro 11.5 is embedded a tool for receptor generation which was used in the mapping out of the coordinate of each target protein receptor complexed with its native co-crystallized ligand.

2.5 Docking Experiment

The docking procedure used in this experiment was carried out using Glide (Grid based ligand docking with energetics) tool v7.5 on Schrodinger maestro (version 2017-1) [20]. The process involves the interaction of the retrieved library of compounds with the active site of the prepared proteins. The co-crystallized ligands and library of compounds were docked with a scaling factor of 0.80 and partial charge cut off of 0.15 into the receptor grid using the standard precision algorithm (SP) leaving the ligand sampling at flexible. Extra precision algorithm (XP) was performed on the glide SP docking protocol with ligand sampling at none (refine only) for further optimization.

2.6 ADMET/Tox Screening

The pharmacokinetics properties of all the retrieved compounds were estimated using qikprop module in maestro 11.5 (QikProp, Schrödinger, 2017-1).

2.7 Validation of Molecular Docking Result

The Accuracy of the docking experiment was validated by extracting the co-crystallized ligands from the proteins, these ligands were prepared using the ligprep tool and docked back into the active site of the protein. All docking protocols were able to replicate the orientation of the ligand to the protein. The RMSD values for each protein to its active site was calculated and they were below 2.5Å.

Table 1. Grid map around the active site of 4M0E, 3TPP and 4ACC proteins

Protein Grid Map	Grid coordinates			Grid Range (Å)	Grid Box ligand range
	X	Y	Z	XYZ	XYZ
4M0E	-17.291	-42.307	25.96	30	10
3TPP	30.513	41.522	2.253	27.212	10
4ACC	17.471	18.86	10.742	27.152	10

3. RESULTS

Table 2. Docked results of showing lead compounds (curcumin and lilacin) of *Aframomum melegueta* leaves phytochemicals against of human acetylcholinesterase, butyrylcholinesterase and GSK-3 beta.

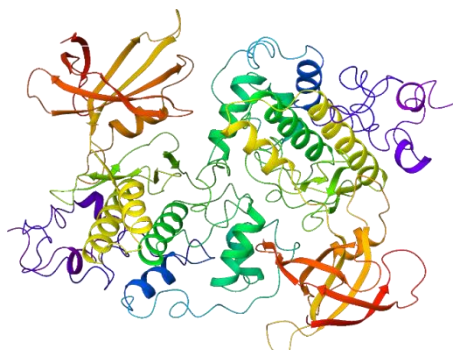
Compound Names	Glide Score (KCAL/MOL)		
	AchE	BchE	GSK-3 β
Co-crystalized ligand	-10.142	-3.890	-6.746
Rivastigmine	-4.837	-8.102	-4.687
Curcumin	-11.203	-9.269	-8.381
Lilacin	-9.694	-9.044	-7.191



a): Human acetylcholinesterase (PDB: 4M0E)



b): Human butyrylcholinesterase (PDB: 6EP4)



c): Human Glycogen Synthase Kinase 3 β (PDB: 4ACC)

Fig. 1. Crystal structures of human Glycogen Synthase Kinase 3 β , butyrylcholinesterase and acetylcholinesterase in ribbon representation

AChe BINDING POSES

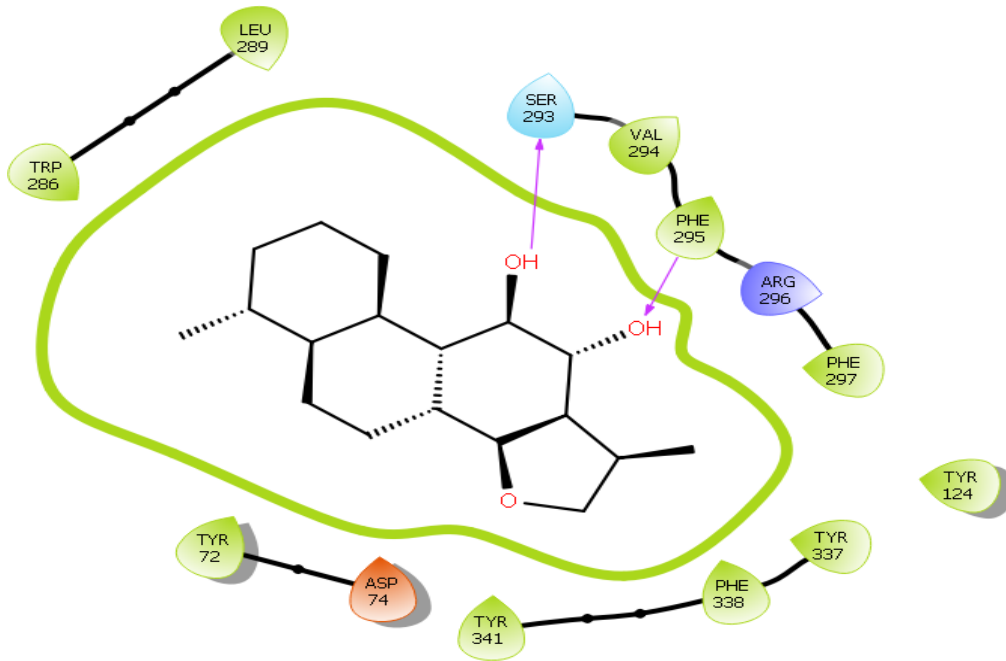


Fig. 4. Binding pose of Co-Crystallized Ligand with human acetylcholinesterase

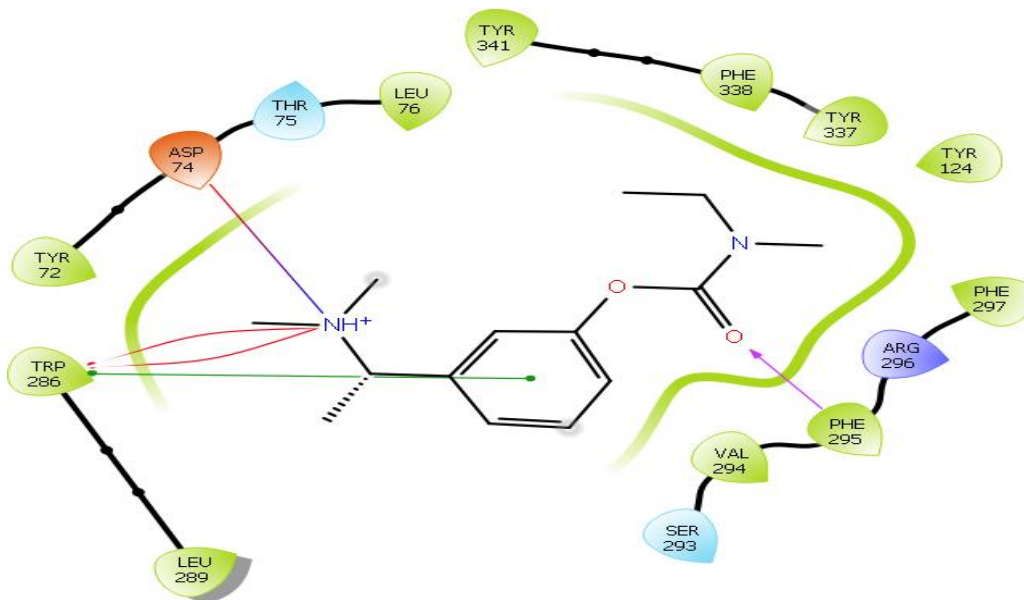


Fig 5. Binding pose of Rivastigmine with human acetylcholinesterase

- | | | | |
|--------------------|----------------------------|--------------------|------------------|
| Charged (negative) | Polar | Distance | Salt bridge |
| Charged (positive) | Unspecified residue | H-bond | Solvent exposure |
| Glycine | Water | Metal coordination | |
| Hydrophobic | Hydration site | Pi-Pi stacking | |
| Metal | Hydration site (displaced) | Pi-cation | |

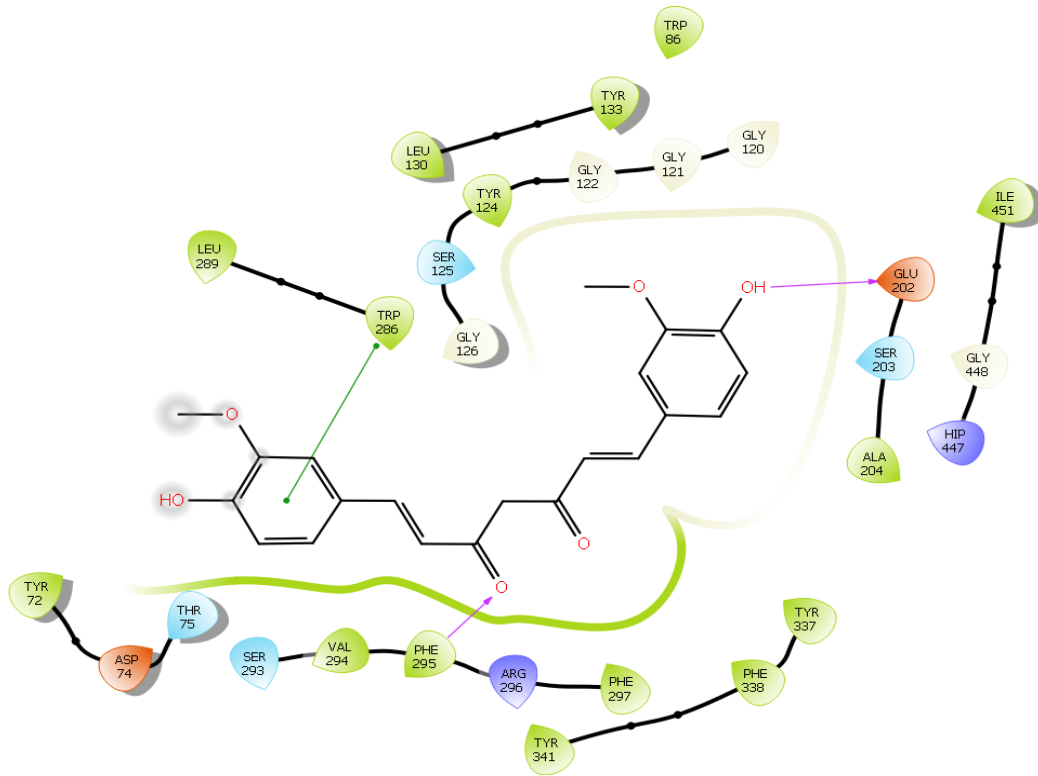


Fig. 6. Binding pose of Curcumin with human acetylcholinesterase

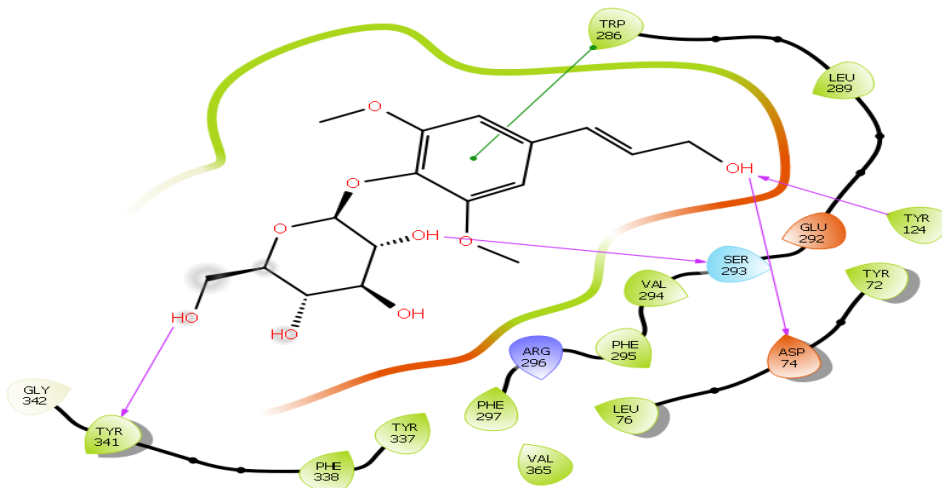


Fig. 7. Binding pose of Lilacin with human acetylcholinesterase

- | | | | |
|--------------------|----------------------------|--------------------|------------------|
| Charged (negative) | Polar | Distance | Salt bridge |
| Charged (positive) | Unspecified residue | H-bond | Solvent exposure |
| Glycine | Water | Metal coordination | |
| Hydrophobic | Hydration site | Pi-Pi stacking | |
| Metal | Hydration site (displaced) | Pi-cation | |

BChe BINDING POSES

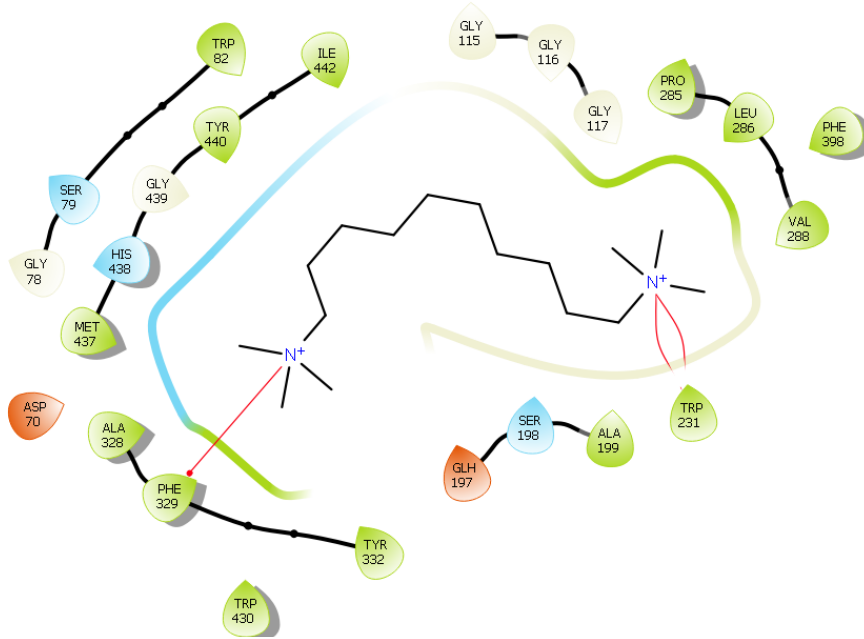


Fig. 8. Binding pose of Co-Crystallized Ligand with Human butyrylcholinesterase

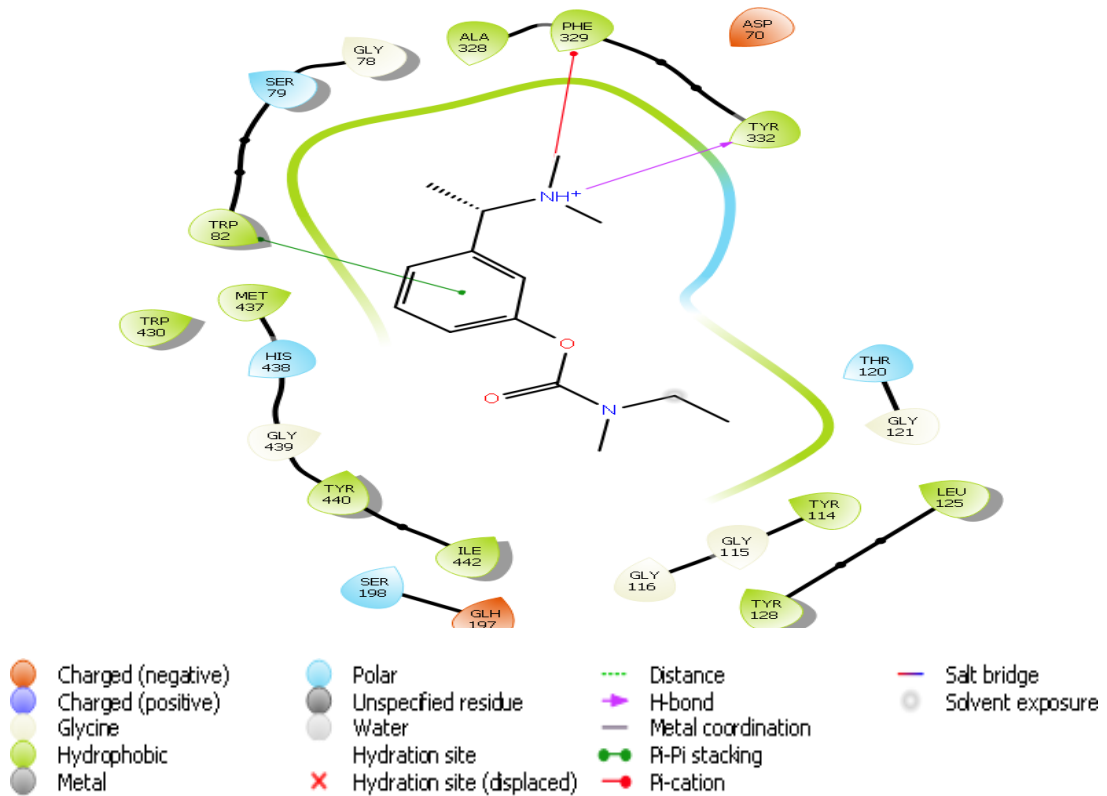


Fig. 9. Binding pose of Rivastigmine with Human butyrylcholinesterase

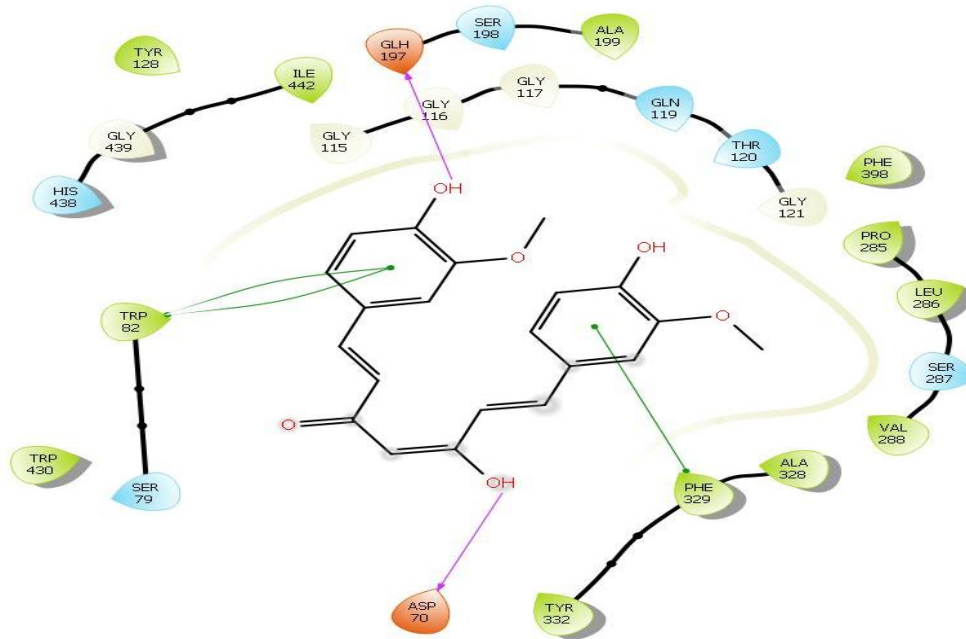


Fig.10. Binding pose of Curcumin with Human butyrylcholinesterase

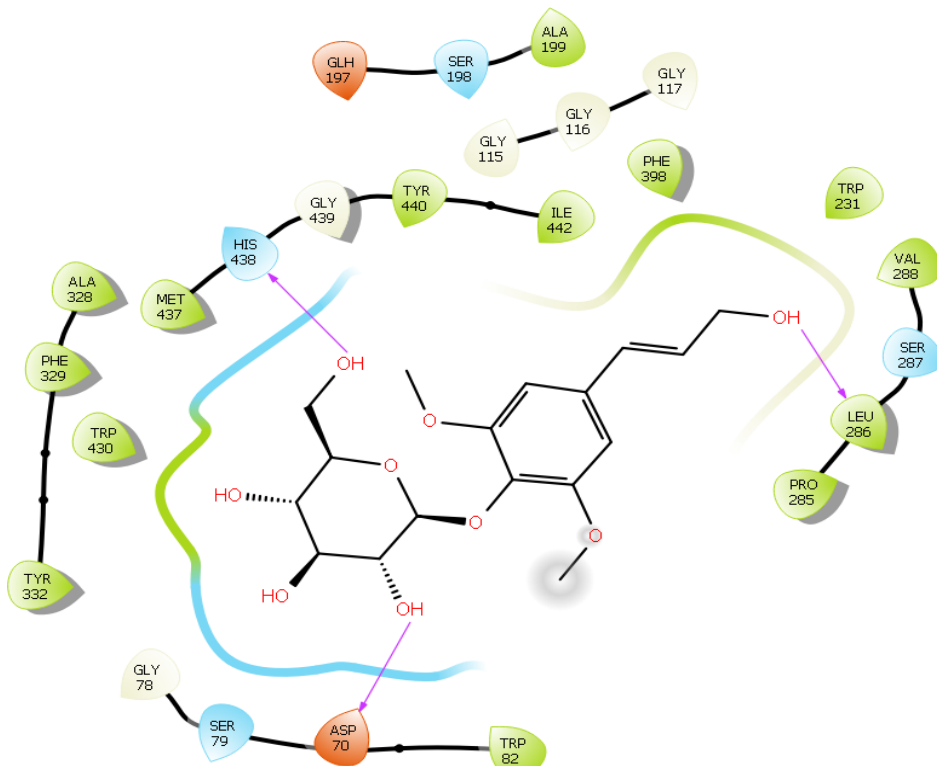


Fig. 11. Binding pose of Lilacin with Human butyrylcholinesterase

- | | | | |
|--------------------|----------------------------|--------------------|------------------|
| Charged (negative) | Polar | Distance | Salt bridge |
| Charged (positive) | Unspecified residue | H-bond | Solvent exposure |
| Glycine | Water | Metal coordination | |
| Hydrophobic | Hydration site | Pi-Pi stacking | |
| Metal | Hydration site (displaced) | Pi-cation | |

GSK-3 β BINDING POSES

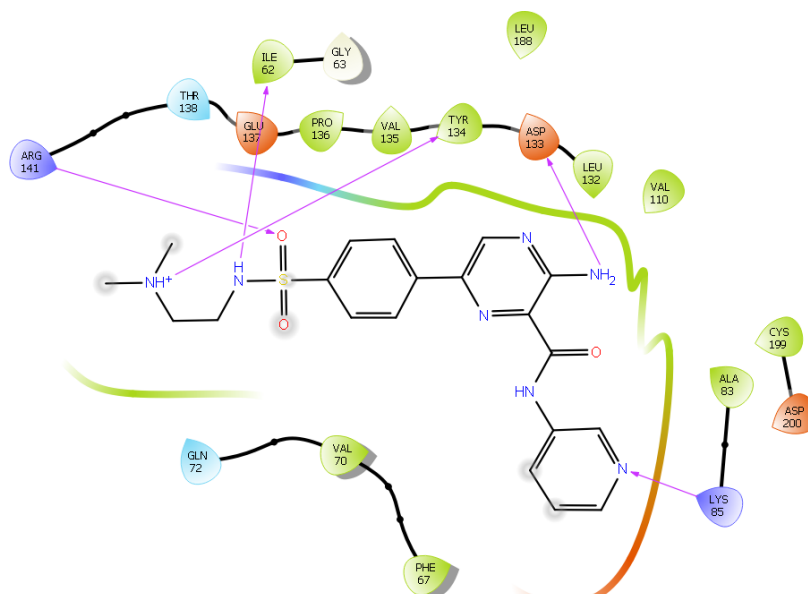


Fig. 12. Binding pose of Co-Crystallized Ligand with human GSK3 β

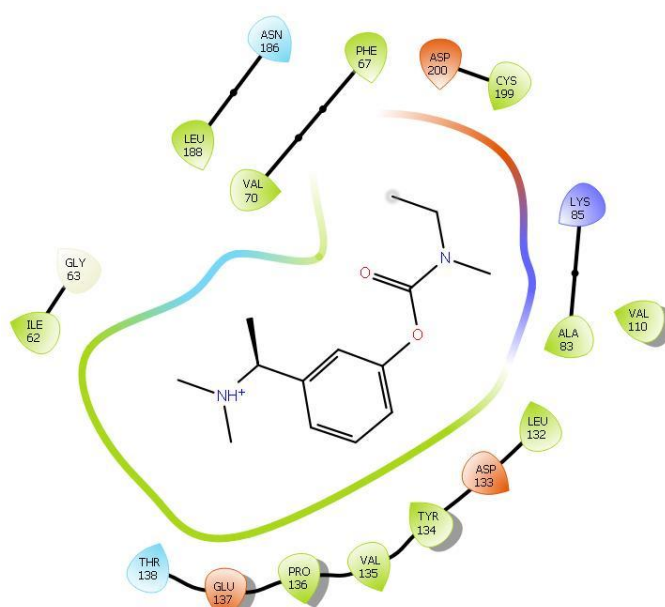


Fig. 13. Binding pose of Rivastigmine with GSK3-beta

- | | | | |
|--------------------|----------------------------|--------------------|------------------|
| Charged (negative) | Polar | Distance | Salt bridge |
| Charged (positive) | Unspecified residue | H-bond | Solvent exposure |
| Glycine | Water | Metal coordination | |
| Hydrophobic | Hydration site | Pi-Pi stacking | |
| Metal | Hydration site (displaced) | Pi-cation | |

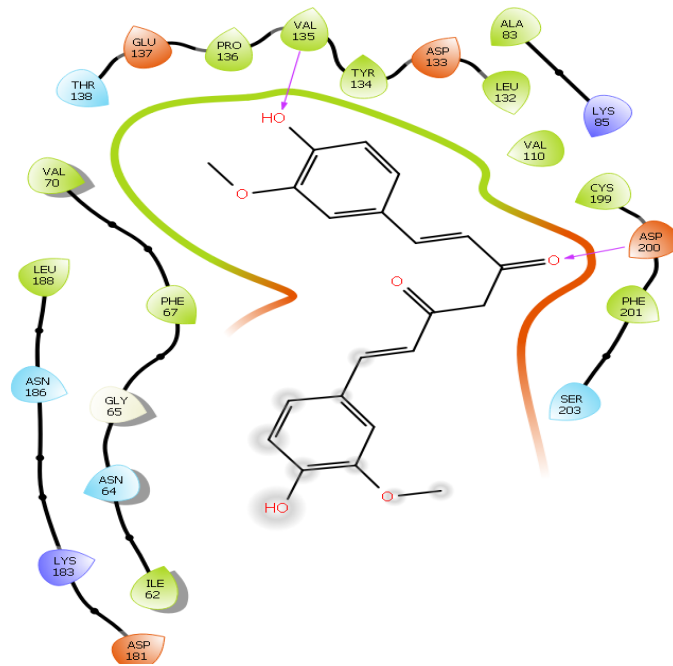


Fig. 14. Binding pose of Curcumin with human GSK3β

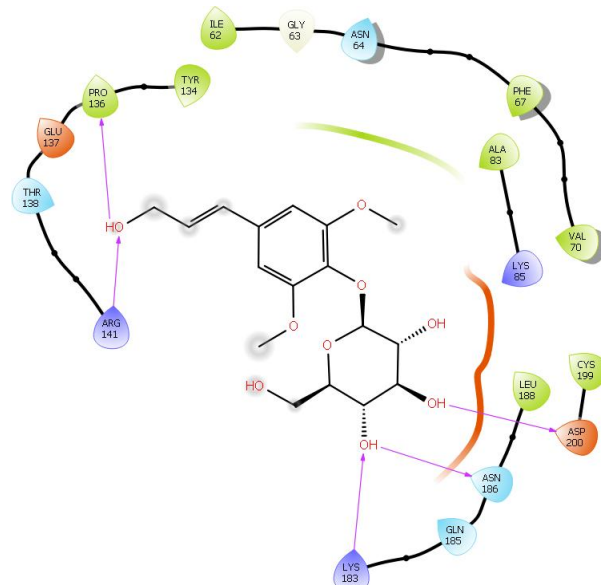


Fig. 15. Binding pose of Lilacin with human GSK3β

- | | | | |
|--|---|--|--|
| ● Charged (negative) | ● Polar | --- Distance | — Salt bridge |
| ● Charged (positive) | ● Unspecified residue | — H-bond | ○ Solvent exposure |
| ● Glycine | ○ Water | — Metal coordination | |
| ● Hydrophobic | ○ Hydration site | ● Pi-Pi stacking | |
| ● Metal | × Hydration site (displaced) | ● Pi-cation | |

Table 3. Admet-tox properties of phytochemicals from *afmomum meleugata* leaves

Compound Names	M.W (g/mol)	donorHB	accptHB	QPlogPo/w	QPlogBB	QPlogKhsa	HOA	ROF
alpha-Cadinol	222.37	1	0.75	4.048	0.151	0.696	3	0
Alpha-Caryophyllene	204.36	0	0	5.185	1.047	0.993	1	1
alpha-Gurjunene	204.36	0	0	5.191	1.111	0.968	1	1
alpha-Murolene	204.36	0	0	5.568	1.059	0.983	1	1
alpha-Selinene	204.36	0	0	5.268	1.008	0.949	1	1
Aromadendrene	204.36	0	0	5.214	1.051	0.973	1	1
beta-Cadinene	204.36	0	0	5.549	1.014	0.979	1	1
beta-Caryophyllene oxide	220.35	0	2	2.487	0.093	0.378	3	0
beta-Caryophyllene	204.36	0	0	5.126	1.039	0.961	1	1
beta-Chamigrene	204.36	0	0	4.989	0.998	0.921	3	0
beta-Cubebene	204.36	0	0	5.518	1.082	1.005	1	1
beta-Elemene	204.36	0	0	5.697	0.995	0.948	1	1
beta-Guaiene	204.36	0	0	5.292	1.113	0.997	1	1
beta-Maaliene	204.36	0	0	4.974	1.085	0.922	3	0
beta-Patchoulene	204.36	0	0	6.551	1.078	0.896	1	1
beta-Selinene	204.36	0	0	5.306	1.011	0.955	1	1
Copaene	204.36	0	0	5.449	1.084	0.959	1	1
Curcumin	368.39	2	7	2.828	-2.246	0.007	2	0
Cyperene	204.36	0	0	4.861	1.074	0.884	3	0
E-Nerolidol	222.37	1	0.75	4.913	-0.2	0.782	3	0
Elemol	222.37	1	0.75	4.204	0.066	0.657	3	0
Elixene	204.36	0	0	5.637	1.048	0.984	1	1
gamma-Cadinene	204.36	0	0	5.554	1.062	0.993	1	1
gamma-Gurjunene	204.36	0	0	5.303	1.063	0.961	1	1
gamma-Murolene	204.56	0	0	5.586	1.062	0.995	1	1
Germacrene D	204.36	0	0	5.474	1.053	0.995	1	1
Gingerol	294.39	1	4.2	3.743	-1.473	0.301	3	0
Humulene Epoxide	220.35	0	2	2.614	0.134	0.435	3	0
Ibuprofen	206.28	1	2	3.497	-0.436	0.057	3	0
Isoaromadendrene Epoxide	220.354	0	2	2.504	0.155	0.383	3	0
Isolimonene	136.24	0	0	4.018	0.796	0.388	3	0
Ledene	204.35	0	0	5.296	1.115	0.987	1	1

Lilacin	372.37	5	12.45	-0.319	-2.304	-0.949	2	0
Linalool	154.25	1	0.75	3.14	0.015	0.135	3	0
Longiborneol	222.37	1	1.7	3.336	0.265	0.424	3	0
Myrtenol	152.24	1	1.7	2.11	0.103	-0.124	3	0
Myrtenyl Acetate	194.27	0	2	2.899	-0.061	0.207	3	0
Octadecenoic acid	282.47	1	2	5.847	-0.9	0.606	3	1
Pinocarvyl Acetate	194.27	0	2	2.977	0.14	0.232	3	0
Spathulenol	220.35	1	0.75	3.931	0.25	0.67	3	0
T-Muurolol	222.37	1	0.75	4.091	0.178	0.703	3	0
trans-Sabinol	152.24	1	1.7	2.271	0.141	-0.07	3	0

M.W: Molecular Weight of compounds (range: 130.0 – 725.0)

DonorHB: Hydrogen Bond donor (range: 0.0 --6.0)

AccptHB: Hydrogen Bond acceptor (range: 2.0 – 20.0)

QPlogPo/w: octanol/water partition coefficient (range: - 2.0 – 6.5)

HOA: Human Oral Absorption. 1, 2, or 3 for low, medium, or high.

QPlogBB: Prediction of blood-brain barrier penetration (range: -3.0 -- 1.2);

QPlogKsha: Prediction of binding to human serum albumin (range: -1.5 to 1.5)

ROF: Rule of Five Violation (range: maximum is 4)

4. DISCUSSION

Age-dependent accumulation of amyloid beta [21,] protein leads to self-association and soluble oligomer formation [54]. Amyloid beta oligomers bind specifically and saturate neurons triggering a variety of changes that result in inhibition of synaptic plasticity [22,23] and concomitant hyperphosphorylation of tau proteins with increased activity of acetyl and butyryl cholinesterases leading to neuronal death. Currently there is no cure for Alzheimer's disease [24] as scientists are working in developing a multi-therapeutic approach in the development of a possible drug for AD cure.

In this work, an *in-silico* technique was used to screen the various phytochemicals from the leaves medicinal plant *Aframomum melegueta* and to see if any of the phytochemicals present in this plant leaves would have a better binding affinity than that Rivastigmine (a standard AChE inhibitor used commercially in Alzheimer's disease treatment) against acetylcholinesterase, butyrylcholinesterase and GSK-3 beta which all proteins that exacerbate the neuronal loss in Alzheimer's disease.

From the molecular docking result, Curcumin and Lilacin are shown to have a higher binding poses than the co-crystallized ligands of either Acetylcholinesterase, Butyrylcholinesterase or GSK-3 beta and the standard drug (Rivastigmine).

The ADMET/Tox properties of compounds Curcumin and Lilacin in the leaves of *Aframomum melegueta* are displayed in Table 3.

According to the Lipinski's rule of five, for a molecule to be drug-like, it should have:

Not more than 5 hydrogen bond donors; curcumin and lilacin contains 2 and 5 hydrogen bond donors respectively thus making both compounds obey this first rule.

- Not more than 10 hydrogen bond acceptors; curcumin and lilacin have 7 and 12.45 hydrogen bond acceptor respectively making only curcumin obey the second rule.
- The molecular weight of the compound should not be more than 500; curcumin

and lilacin having a molecular weight of 368.385 and 372.371 respectively.

- A partition co-efficient Log P (a measure of lipophilicity) of less than 5; curcumin and lilacin having 2.828 and -0.319, thus making them obey the rule.
- The last rule states that the compound will be a useful compound for drug development once it doesn't violate more than one of the rules.

Pardridge [25] also stated that the ability of compounds to pass the blood brain barrier must be considered when screening and designing drugs against neurodegenerative diseases, two out the factors to consider are the molecular weights of the compounds (range 179 – 380 Da) and the log BB (range: -3.0 -- 1.2).

The results from Table 3 shows that the molecular weights and the log BB values of curcumin and lilacin are within the accepted range and will pass through the blood brain barrier into the brain and elicit their pharmacological function (inhibit acetylcholinesterase, butyrylcholinesterase and GSK3 beta).

5. CONCLUSION

Plant phytochemical extracts have showed important role in treating and preventing human diseases particularly those that are of increased prevalence such as Alzheimer's disease. Here, based on this *in silico* studies, it is proposed that the inhibiting activity of the phytochemical constituents from the leaves of the plant *Aframomum melegueta* particularly the lead compounds curcumin and lilacin showed the highest docking scores against acetylcholinesterase, butyrylcholinesterase and GSK-3 beta suggesting potent compounds in Alzheimer's disease therapy. The pharmacokinetics studies also showed that curcumin and lilacin have drug-like properties and will most likely pass through the blood brain barrier into the brain.

However, further *in vitro* blood barrier models are needed to be performed to confirm the ability of curcumin and lilacin to pass through the blood brain barrier and also *in vivo* experiments should be carried out to establish the pharmacological activities of curcumin and lilacin in the development of Alzheimer disease multi-dimensional therapy.

CONSENT

As per international standard or university standard, patients' written consent has been collected and preserved by the author(s).

ETHICAL APPROVAL

As per international standard or university standard written ethical approval has been collected and preserved by the author(s).

COMPETING INTERESTS

Authors have declared that no competing interests exist.

REFERENCES

1. Gatz M, Reynolds CA, Fratiglioni L, Johansson B, Mortimer JA, Berg S, Fiske A, and Pedersen, NL. "Role of genes and environments for explaining Alzheimer disease". *Archives of General Psychiatry*. 2006;**63**(2):168–74.
2. Jeon SG, Song EJ, Lee D, Park J, Nam Y, Kim JI, Moon M. Traditional Oriental Medicines and Alzheimer's Disease. *Aging and Disease*. 2019;**10**(2):307–328. Available: <https://doi.org/10.14336/ad.2018.0328>
3. Kabir MT, Uddin MS, Mamun AA, Jeandet P, Aleya L, Mansouri RA, Ashraf GM, Mathew B, Bin-Jumah MN, Abdel-Daim MM. Combination Drug Therapy for the Management of Alzheimer's Disease. *International Journal of Molecular Sciences*. 2020;**21**(9):3272. Available: <https://doi.org/10.3390/ijms21093272>
4. Knippers RHM, Gallois S, van Andel T. (). Commercialization of *Aframomum* spp. in Africa: a Systematic Review of Literature and Supporting Botanical Vouchers. *Econ Bot*. 2021;**75**:76–91. Available: <https://doi.org/10.1007/s12231-021-09517-4>.
5. Osuntokun OT, Olumekun VO, Ajayi AO, Omotuyi IO, Olonisakin A. Assessment of in-vitro Antioxidant/Enzymes Inhibitory Potentials *Aframomum melegueta* [Roscoe] K. Schum (Grains of Paradise) Leaf, Stem Bark, Seed Bark and Seed Extracts. *Archives of Current Research International*. 2020;**20**(2):40-57. Available: <https://doi.org/10.9734/acri/2020/v20i230176>
6. Haake A, Nguyen K, Friedman L, Chakkamparambil B, Grossberg GT. An update on the utility and safety of cholinesterase inhibitors for the treatment of Alzheimer's disease. *Expert Opinion on Drug Safety*. 2020;**19**(2):147–157.
7. Hampel H, Caraci F, Cuello AC, Caruso G, Nisticò R, Corbo M, Baldacci F, Toschi N, Garaci F, Chiesa PA, Verdooner SR, Akman-Anderson L, Hernández F, Ávila, J, Emanuele E, Valenzuela PL, Lucía A, Watling M, Imbimbo BP, Vergallo A, Lista S. A Path Toward Precision Medicine for Neuroinflammatory Mechanisms in Alzheimer's Disease. *Frontiers in Immunology*. 2020;**11**:456.
8. Greenwood JR, Calkins D, Sullivan AP, Shelley JC. Towards the comprehensive, rapid, and accurate prediction of the favorable tautomeric states of drug- like molecules in aqueous solution. *Journal of computer-aided molecular design*, 2010;**24**(6-7):591- 604
9. Sharma K. Cholinesterase inhibitors as Alzheimer's therapeutics (Review) *Molecular Medicine Reports*, 2019;**20**:1479-1487. Available: <https://doi.org/10.3892/mmr.2019.10374>
10. Darvesh S. Butyrylcholinesterase as a Diagnostic and Therapeutic Target for Alzheimer's Disease. *Current Alzheimer Research*. 2016;**13**(10):1173–1177.
11. Hooper C, Killick R, Lovestone S. The GSK3 hypothesis of Alzheimer's disease. *J. Neurochem*. 2008;**104**:1433–1439.
12. Muyliaert D, Kremer A, Jaworski T, Borghgraef P, Devijver H, Croes S, et al. Glycogen synthase kinase-3 β , or a link between amyloid and tau pathology? *Genes Brain Behav*. 2008;**7**:57–66.
13. Abdellatif M, Ali A, Ali A, Hussien M. Computational studies by molecular docking of some antiviral drugs with COVID-19 receptors are an approach to medication for COVID-19. *Open Chemistry*. 2021;**19**(1):245-246.
14. Butt S, Badshah Y, Shabbir M, Rafiq M. Molecular Docking Using Chimera and Autodock Vina Software for

- Nonbioinformaticians, JMIR Bioinform Biotech. 2020;1(1):e14232. DOI: 10.2196/14232.
15. Lengauer T, Rarey M. "Computational methods for biomolecular docking". Current Opinion in Structural Biology. 1996;6(3):402–6.
 16. Müller T. Rivastigmine in the treatment of patients with Alzheimer's disease. Neuropsychiatric Disease and Treatment. 2007;3 (2): 211–218.
 17. Sastry GM, Adzhigirey M, Day T, Annabhimoju R, Sherman W. Protein and ligand preparation: parameters, protocols, and influence on virtual screening enrichments. Journal of Computer-aided Molecular Design. 2013;27(3):221-234.
 18. Greenwood JR, Calkins D, Sullivan AP, Shelley JC. Towards the comprehensive, rapid, and accurate prediction of the favorable tautomeric states of drug- like molecules in aqueous solution. Journal of Computer-aided Molecular Design. 2010;24(6-7):591- 604.
 19. Owokotomo I, Ekundayo O, Oguntuase B. Chemical Constituents of the Leaf, Stem, Root and Seed Essential Oils of Aframomum melegueta (K. Schum) from South West Nigeria. International Research Journal of Pure and Applied Chemistry. 2014;4:395-401.
 20. Friesner RA, Murphy RB, Repasky MP, Frye LL, Greenwood JR, Halgren TA, Mainz DT. Extra precision glide: Docking and scoring incorporating amodel of hydrophobic enclosure for protein-ligand complexes. Journal of Medicinal Chemistry. 2006;49(21):6177- 6196.
 21. Selkoe DJ, Hardy J. The amyloid hypothesis of Alzheimer's disease at 25 years. EMBO Mol Med. 2016;8:595–608.
 22. Lesne SE, Sherman MA, Grant M, Kuskowski M, Schneider JA. Brain amyloid- beta oligomers in ageing and Alzheimer's disease. Brain. 2013;136:1383.
 23. Zempel H, Luedtke J, Kumar Y, Biernat J, Dawson H. Amyloid-beta oligomers induce synaptic damage via Tau-dependent microtubule severing by TTL6 and spastin. EMBO J. 2013;32:2920–2937.
 24. Yiannopoulou KG, Papageorgiou SG. Current and Future Treatments in Alzheimer Disease: An Update. Journal of Central Nervous System Disease. 2020;12:1179573520907397. Available:https://doi.org/10.1177/11795735 20907397
 25. Pardridge WM. Treatment of Alzheimer's Disease and Blood-Brain Barrier Drug Delivery. Pharmaceuticals (Basel, Switzerland), 2020;13(11):394.

© 2022 Oluwadahunsi et al.; This is an Open Access article distributed under the terms of the Creative Commons Attribution License (<http://creativecommons.org/licenses/by/4.0>), which permits unrestricted use, distribution, and reproduction in any medium, provided the original work is properly cited.

Peer-review history:

The peer review history for this paper can be accessed here:
<https://www.sdiarticle5.com/review-history/84242>